JACC: CARDIOONCOLOGY VOL. 2, NO. 2, 2020

ORIGINAL RESEARCH

Computed Tomographic Angiography Assessment of Epicardial Coronary Vasoreactivity for Early Detection of Doxorubicin-Induced Cardiotoxicity

Attila Feher, MD, PhD,[a,b,*] Nabil E. Boutagy, PhD,[a,b,*] John C. Stendahl, MD, PhD,[a,b] Christi Hawley,[b] Nicole Guerrera, RDCS,[b] Carmen J. Booth, DVM, PhD,[c] Eva Romito, PhD,[a,b] Steven Wilson, VMD,[c] Chi Liu, PhD,[d] Albert J. Sinusas, MD[a,b,d,e]

ABSTRACT

BACKGROUND The vascular endothelium is a novel target for the detection, management, and prevention of doxorubicin (DOX)-induced cardiotoxicity.

OBJECTIVES The study aimed to: 1) develop a methodology by computed tomography angiography (CTA) to evaluate stress-induced changes in epicardial coronary diameter; and 2) apply this to a chronic canine model of DOX-induced cardiotoxicity to assess vascular toxicity.

METHODS To develop and validate quantitative methods, sequential retrospectively gated coronary CTAs were performed in 16 canines. Coronary diameters were measured at prespecified distances during rest, adenosine (ADE) (280 μg/kg/min), rest 30 min post-ADE, and dobutamine (DOB) (5 μg/kg/min). A subgroup of 8 canines received weekly intravenous DOX (1 mg/kg) for 12 to 15 weeks, followed by rest-stress CTA at cumulative doses of ∼4-mg/kg (3 to 5 mg/kg), ∼8-mg/kg (7 to 9 mg/kg), and ∼12-mg/kg (12 to 15 mg/kg) of DOX. Echocardiograms were performed at these timepoints to assess left ventricular ejection fraction and global longitudinal strain.

RESULTS Under normal conditions, epicardial coronary arteries reproducibly dilated in response to ADE (left anterior descending coronary artery [LAD]: 12 ± 2%, left circumflex coronary artery [LCx]: 13 ± 2%, right coronary artery [RCA]: 14 ± 2%) and DOB (LAD: 17 ± 3%, LCx: 18 ± 2%, RCA: 15 ± 3%). With DOX, ADE vasodilator responses were impaired after ∼4-mg/kg (LAD: −3 ± 1%, LCx: 0 ± 2%, RCA: −5 ± 2%) and ∼8-mg/kg (LAD: −3 ± 1%, LCx: 0 ± 1%, RCA: −2 ± 2%). The DOB dilation response was preserved at ∼4-mg/kg of DOX (LAD: 18 ± 4%, LCx: 11 ± 3%, RCA: 11 ± 2%) but tended to decrease at ∼8-mg/kg of DOX (LAD: 4 ± 2%, LCx: 8 ± 3%, RCA: 3 ± 2%). A significant left ventricular ejection fraction reduction was observed only at 12 to 15 mg/kg DOX (baseline: 63 ± 2%, 12-mg/kg: 45 ± 3%). Global longitudinal strain was abnormal at ∼4-mg/kg of DOX ($p = 0.011$).

CONCLUSIONS CTA can reliably assess epicardial coronary diameter in response to pharmacological stressors, providing a noninvasive functional index of coronary vasoreactivity. Impaired epicardial vasodilation occurs early in DOX-induced cardiotoxicity. (J Am Coll Cardiol CardioOnc 2020;2:207–19) © 2020 Published by Elsevier on behalf of the American College of Cardiology Foundation. This is an open access article under the CC BY-NC-ND license (http://creativecommons.org/licenses/by-nc-nd/4.0/).

From the [a]Section of Cardiovascular Medicine, Department of Internal Medicine, Yale University School of Medicine, New Haven, Connecticut, USA; [b]Yale Translational Research Imaging Center, Yale University, New Haven, Connecticut, USA; [c]Department of Comparative Medicine, Yale University School of Medicine, New Haven, Connecticut, USA; [d]Department of Radiology and Biomedical Imaging, Yale University School of Medicine, New Haven, Connecticut, USA; and the [e]Department of Biomedical Engineering, Yale University School of Medicine, New Haven, Connecticut, USA. *Drs. Feher and Boutagy contributed equally to this work. This work was supported by the National Institute of Health grants HL123949 (to Dr. Liu), HL098069 (to Dr. Sinusas),

ISSN 2666-0873 https://doi.org/10.1016/j.jaccao.2020.05.007

ABBREVIATIONS AND ACRONYMS

ADE = adenosine

CAD = coronary artery disease

CTA = computed tomography angiography

DOB = dobutamine

DOX = doxorubicin

GLS = global longitudinal strain

HR = heart rate

LAD = left anterior descending coronary artery

LCx = left circumflex coronary artery

LV = left ventricular

LVEF = left ventricular ejection fraction

MAP = mean arterial pressure

RCA = right coronary artery

TTE = transthoracic echocardiography

Early screening strategies and therapeutic advances have dramatically reduced cancer-related mortality (1). However, increased life expectancy of cancer patients comes at a cost of increased risk for treatment-related cardiovascular morbidity and mortality (2). Relevant to this issue, doxorubicin (DOX) is a frequently used and effective chemotherapeutic agent but is associated with cardiotoxicity in treated individuals (3). DOX-induced cardiotoxicity usually presents as systolic dysfunction, which develops in a dose-dependent manner and can progress to heart failure (4). The development of cardiotoxicity can necessitate the modification of the anticancer regimen, which may lead to suboptimal oncologic treatment. Importantly, DOX-induced cardiotoxicity can be irreversible, although recent studies suggest that early cardiotoxicity detection coupled with prompt initiation of guideline-directed heart failure medical therapy can result in improvements in left ventricular (LV) systolic function (5,6).

For screening purposes, current guidelines recommend serial assessment of LV ejection fraction (LVEF) by transthoracic echocardiography (TTE) or cardiac magnetic resonance (7). Notably, a reduction in LVEF is considered a late finding in DOX-induced cardiotoxicity, as patients can have histological evidence of myocardial injury on biopsy before reduction in LVEF (8).

General heart failure guidelines recommend that coronary artery disease (CAD) should be considered as a potential etiology in patients with new diagnosis of impaired LVEF. Coronary computed tomography angiography (CTA) may be employed to detect and localize large-vessel coronary obstructions (9). Indeed, CTA has been shown to be a highly sensitive and specific tool for detecting CAD in patients with dilated cardiomyopathy (10,11). CTA may be utilized in patients with a prior history of chemotherapy and new onset LV dysfunction to exclude underlying CAD. Along these lines, a study investigating 80 cancer patients showed that CTA findings altered the therapeutic strategy in 52% of patients by aiding in the decision of withholding, altering, or continuing oncologic therapy (12). In addition to anatomical information, CTA can also offer physiological data with respect to cardiac function and myocardial perfusion. Although not routinely assessed by CTA, stressor-induced changes in epicardial coronary diameter may provide additional information about vascular reactivity.

Preclinical studies suggest that DOX administration is associated with microvascular damage by inducing oxidative stress (13,14) or direct DNA damage in endothelial cells (15). Other studies indicate that DOX can also interfere with important vasoactive pathways, such as nitric oxide bioavailability and signaling (16). Indeed, disruption of endothelial signaling pathways has been shown to cause functional impairments in the myocardium (17). Along these lines, targeting endothelial inflammation or angiogenesis in rodent models of DOX induced-cardiotoxicity successfully prevented DOX-induced cardiotoxicity by ameliorating endothelial damage (18,19). Based on these and other studies, the vascular endothelium is emerging as a novel target for improving the detection, management, and prevention of DOX-induced cardiotoxicity (20).

The aims of the present study were 2-fold: 1) to test whether CTA could provide a reliable, quantitative assessment of epicardial coronary diameter during pharmacological stress with adenosine (ADE) and low-dose dobutamine (DOB); and 2) to apply quantitative serial rest-stress CTA analysis of coronary vessel reactivity in a chronic canine model of DOX-induced cardiotoxicity.

METHODS

CANINE EXPERIMENTS. Sixteen retired-breeder purpose-bred female Marshall beagles (weight ~10 kg; Marshall BioResources, North Rose, New York) dogs were used for this project. All experiments were performed in accordance with Yale University Institutional Animal Care and Use Committee standards and approval, and according to the National Institutes of Health Guidelines for Care and Use of Laboratory Animals. All dogs were acclimated to their new

and S10RR025555 (to Dr. Sinusas). The authors have reported that they have no relationships relevant to the contents of this paper to disclose.

The authors attest they are in compliance with human studies committees and animal welfare regulations of the authors' institutions and Food and Drug Administration guidelines, including patient consent where appropriate. For more information, visit the *JACC: CardioOncology* author instructions page.

Manuscript received March 15, 2020; revised manuscript received May 8, 2020, accepted May 11, 2020.

FIGURE 1 Study Timeline

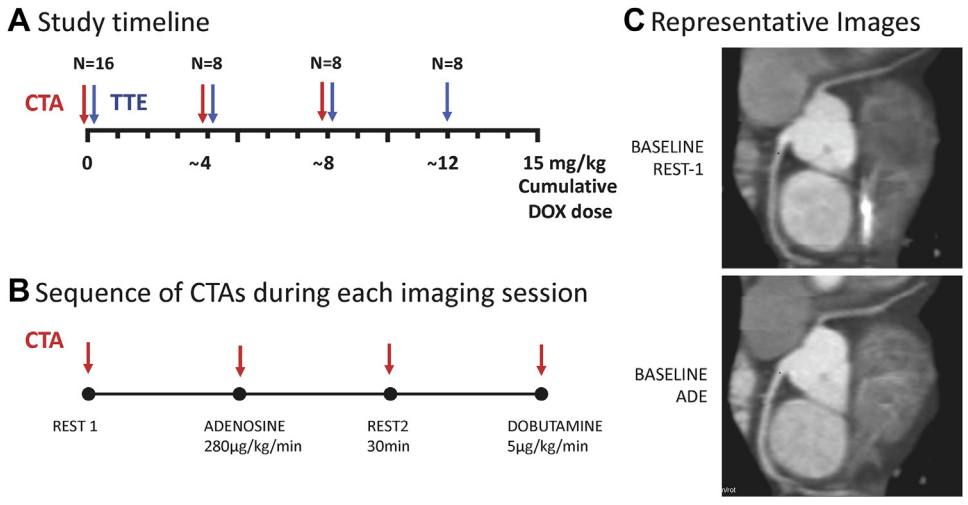

A group of canines (n = 8) were administered doxorubicin (DOX) (1 mg/kg) weekly for 12–15 weeks. **(A)** Serial contrast coronary computed tomography angiography (CTA) was performed at baseline, and after ~4-mg/kg and ~8-mg/kg cumulative dose of doxorubicin (DOX), as indicated by the **red arrows**. Transthoracic echocardiography (TTE) was performed at baseline, and after ~4-, ~8- and ~12-mg/kg cumulative DOX doses, as indicated by the **blue arrows**. **(B)** The sequence of each rest and pharmacological stress CTA imaging session. **(C)** Representative multiplanar reformatted CTA images acquired at REST-1 and after administration of adenosine (ADE).

environment and were fed a standard diet for at least 5 days prior to performing any procedures. Before each CTA session, dogs were sedated with propofol (5 to 7.5 mg/kg) via intravenous injection in the cephalic vein, and then were rapidly intubated for mechanical ventilation (Venturi, Cardiopulmonary Corp., Milford, Connecticut) and anesthesia maintenance. Anesthesia was maintained with 1.0% to 2.0% isoflurane, 55% to 60% nitrous oxide, and 40% to 45% oxygen. The level of anesthesia was monitored and adjusted based on heart rate (HR), blink reflex, and jaw tone. Blood gases, electrolytes, and hematocrit (VetStat Electrolyte and Blood Gas Analyzer, IDEXX Laboratories, Westbrook, Maine), as well as expired CO_2, were measured throughout the study, and ventilator settings were adjusted accordingly to maintain gases within physiological limits. Cardiac rhythm and rate, oxygen saturation, and body temperature (rectal temperature probe) were continuously monitored (Philips IntelliVue MP50 monitor, Philips Healthcare, Andover, Massachusetts). Following a small femoral cutdown (4 cm), a 5-F introducer sheath was placed in the femoral artery for arterial blood sampling and blood pressure measurements. Femoral artery pressures were continuously measured with a fluid-filled catheter (Transpac IV, ICU Medical, San Clemente, California) connected to a Bridge Amp (AD Instruments, Sydney, Australia) that was interfaced with a PowerLab (AD instruments) data acquisition system. Cardiac rhythm and rate and pressures were continuously monitored throughout the experiment with a dedicated workstation and software package (LabChart 8.0, AD Instruments) that was also used for subsequent offline data analysis. Intravenous fluids were administered through cephalic and femoral vein access. Intramuscular Nubain (0.14 to 0.20 mg/kg, given every 12 h for 72 h) was used for postoperative analgesia after every invasive procedure.

CANINE MODEL OF DOX-INDUCED CARDIOTOXICITY. Following baseline imaging, a subgroup of canines (n = 8) had a vascular access port (Access Technologies, Albuquerque, New Mexico) placed in the subcutaneous space between the scapulae on the dorsal midline with the tip of the catheter positioned within the cavoatrial junction. Following recovery, these canines were treated with 1-mg/kg DOX (Sagent Pharmaceuticals, Schaumberg, Illinois) weekly for 12 to 15 weeks via sterile technique (total cumulative dose of DOX: 260 to 325 mg/m^2) as previously described (21). Complete blood count was assessed prior to each DOX administration, and DOX dosing was delayed for absolute neutrophil count values <1,500. To manage the potential side effects of

FIGURE 2 Plots of Correlation and Agreement Between REST-1 and REST-2 Diameters

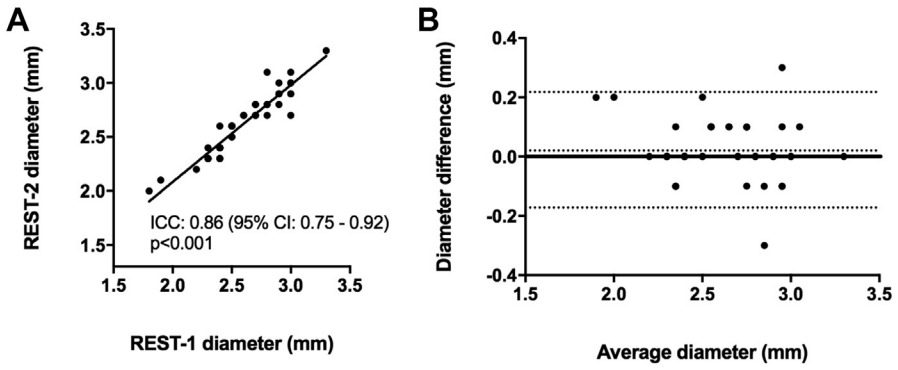

(A) Correlation between REST-1 and REST-2 coronary diameters, including all baseline analyzed coronary segments (n = 48 pairs). Please note that in case of identical diameter values, the data points may overlap. **(B)** Bland-Altman plot analysis including all baseline REST-1 and REST-2 coronary diameters (n = 48 pairs). The **solid line** represents zero, the **central dashed line** indicates bias, and the 2 **outer dashed lines** indicate the 95% limits of agreement. CI = confidence interval; ICC = intraclass correlation coefficient.

DOX administration, animals were administered daily prophylactic enrofloxacin (5 mg/kg orally; Bayer Animal Health, Leverkusen, Germany) and as needed ondansetron (0.8 mg/kg orally; Hospira, Lake Forest, Illinois) for nausea. LV function was measured serially at ~4-mg/kg (3 to 5 mg/kg), ~8-mg/kg (7 to 9 mg/kg), and ~12-mg/kg (12 to 15 mg/kg) cumulative DOX dose by TTE (Philips iE33) in awake animals. LVEF and intracardiac volumes were calculated by using the modified biplane Simpson method using dedicated system software. Wall thickness and LV diameter was obtained from parasternal long axis view. In addition, 2-dimensional strain analysis was performed with previously validated commercial software (EchoInsight, Research Version 2.2.5, Epsilon, Weaverville, North Carolina) (22) to derive global longitudinal strain (GLS). To validate our model of anthracycline-induced cardiotoxicity and assess timing of myocardial injury, we performed histopathological analyses in serial endomyocardial biopsies and terminal autopsy specimens. Accordingly, in a subset of DOX-treated dogs (n = 4), LV endomyocardial biopsies were collected under fluoroscopic guidance at ~4- and ~8-mg/kg cumulative DOX doses using a bioptome (Argon Medical, Frisco, Texas) guided through a long guide inserted via the right femoral artery access. At the end of the last imaging session, animals were euthanized under deep anesthesia (5% isoflurane) via intravenous injection of saturated potassium chloride following a heparin bolus (20,000 U). After the confirmation of death, tissue specimens were collected from the LV myocardium. The study timeline is depicted in Figure 1A.

CORONARY CTA. Sequential CTAs were performed under general anesthesia using a hybrid 64-slice single-photon emission CT/CT (Discovery NM570c, GE Healthcare, Milwaukee, Wisconsin) with detector collimation of 64 × 0.6 mm. In the DOX treatment group, CTA was performed 4 to 6 days after DOX dosing. Retrospectively gated CTAs (120 kV, 350 mA) were acquired after iodinated contrast administration (iohexol, 350 mg/ml, average: 13 ml, 2 ml/s) without intravenous nitroglycerin. Sequential CTAs were performed at rest (REST-1), during ADE infusion (280 μg/kg/min), repeated at rest 30 min after discontinuation of ADE (REST-2), and during low-dose DOB infusion (5 μg/kg/min) (Figure 1B). Before DOB studies, a ramping protocol was used to achieve target DOB dosing (DOB infusion was started at 1.25 μg/kg/min, up-titrated initially to 2.5 μg/kg/min after 5 min, and then up-titrated to the final 5 μg/kg/min after additional 5 min). Images were reconstructed at 70% to 80% of the cardiac cycle using filtered back projection and a standard kernel (GE Healthcare) (Figure 1C). Cross-sectional proximal luminal diameters were measured at preset distances (3 to 6 mm depending on coronary anatomy) from vessel origins using reformatted 0.6-mm-thick cross-sectional

FIGURE 3 Hemodynamic Analysis

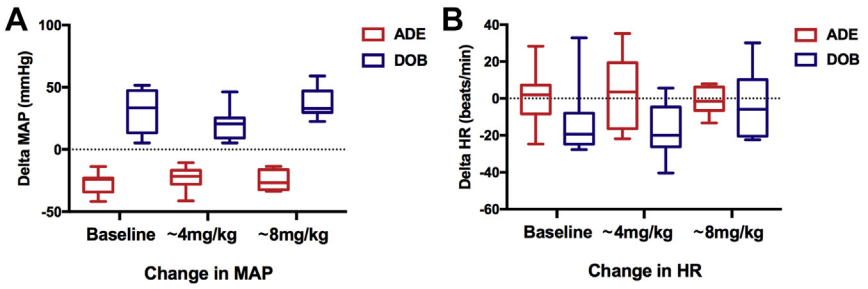

Change in **(A)** mean arterial pressure (MAP) and **(B)** heart rate (HR) compared with resting values in response to adenosine (ADE) and dobutamine (DOB). The **boxes** represent the 25th to 75th percentiles, the **midlines** represent the median values, and the **whiskers** indicate minimal and maximal values, n = 8 for each group.

multiplanar images perpendicular to the vessel centerline using system software (GE AW VolumeShare 5 software, GE Healthcare).

HISTOPATHOLOGICAL ANALYSES OF MYOCARDIUM. LV cardiac biopsies and sections of heart following euthanasia were divided and immersion-fixed for histology in 10% neutral buffered formalin. Paraffin-embedded sections (3 to 5 μm) were stained with hematoxylin and eosin by routine methods (Comparative Pathology Research, Comparative Medicine, School of Medicine, Yale University). Hematoxylin and eosin-stained sections were evaluated for the presence and severity of myocardial toxicity by a veterinarian (C.J.B.) trained in veterinary pathology with extensive expertise in canine pathology, blinded to the experimental time point. LV sections were scored by previously established 5-point semiquantitative analysis system (23) modified based on prior DOX-induced cardiotoxicity rodent studies (24). LV sections were scored by individual parameters: myocardial inflammation and cardiac myocyte: vacuolation, edema, sarcoplasmic fragmentation or loss of striation, degeneration, hypereosinophilic, and nuclear hypertrophy and nuclear pyknosis. A summed myocardial toxicity severity score was calculated by summing the individual scores.

STATISTICAL ANALYSIS. Statistical analyses were performed with GraphPad Prism Software 7 (GraphPad Software, San Diego, California) and IBM SPSS Statistics (version 1.0.0.1327, Armonk, New York). Normality of the data was assessed by using the D'Agostino-Pearson omnibus normality test. Group means were compared using 1- or 2-way analysis of variance using repeated measures when appropriate. Post hoc analyses were performed with a Sidak multiple comparisons test. The intraclass correlation coefficient with 95% confidence interval was calculated, and Bland-Altman plot analysis was performed to evaluate the relationship and agreement between REST-1 and REST-2 diameters (16 animals × 3 vascular segments = 48 data point pairs). The coronary measurements were analyzed by comparison with their respective baselines; for example, ADE diameters were compared with REST-1 diameters and DOB diameters were compared with REST-2 diameters. All data are expressed as mean ± SEM. The significance level was set a priori at $p < 0.05$.

RESULTS

BASELINE STUDIES UNDER NORMAL CONDITIONS. In 16 canines, under normal conditions, ADE decreased mean arterial pressure (MAP) (-27 ± 3 mm Hg) with no significant change in HR (1 ± 5 beats/min), while DOB increased MAP (53 ± 6 mm Hg) and decreased HR (-13 ± 7 beats/min). All major epicardial coronary arteries dilated significantly in response to ADE (left anterior descending coronary artery [LAD]: 12 ± 2%, left circumflex coronary artery [LCx]: 13 ± 2%, right coronary artery [RCA]: 14 ± 2%) (Supplemental Table 1). Similarly, DOB induced significant coronary dilation in all vascular segments (LAD: 17 ± 3%, LCx: 18 ± 2%, RCA: 15 ± 3%). Importantly, rest diameter measurements were highly reproducible between rest studies (LAD: 1 ± 2%, LCx: 1 ± 2%, RCA: 1 ± 2%), as demonstrated by a good correlation between REST-1 and REST-2 diameters

FIGURE 4 Serial Echocardiographic Analysis

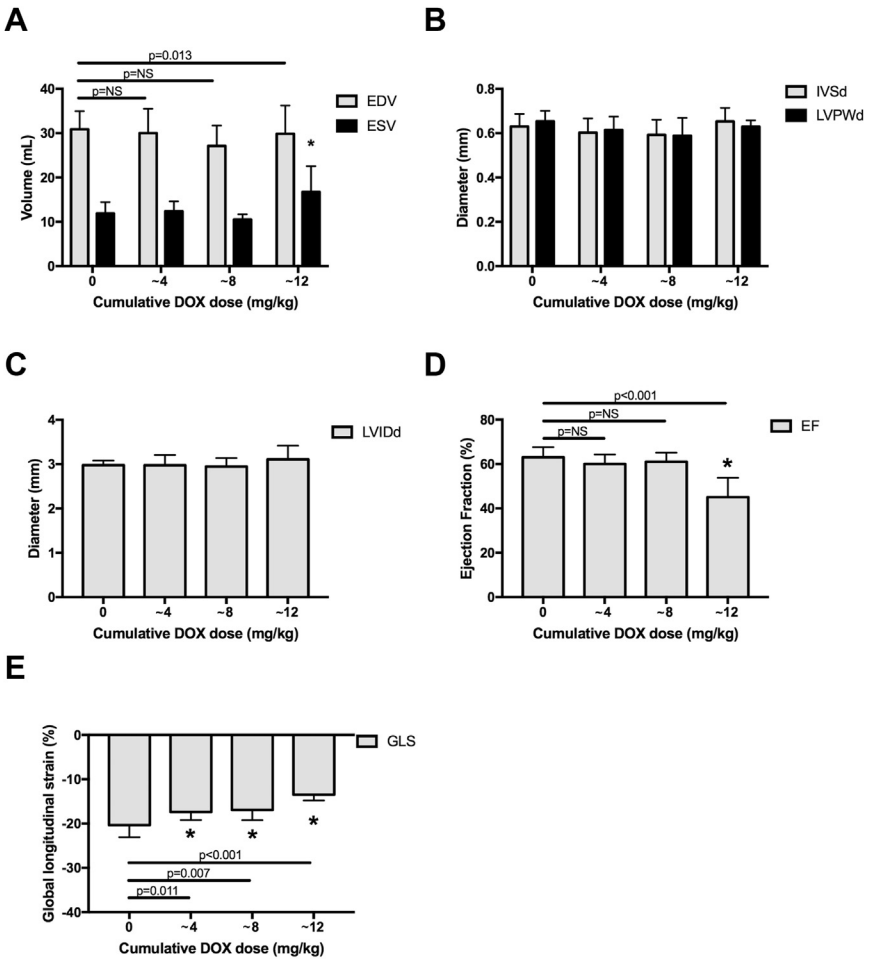

(A) End-diastolic volume (EDV) and end-systolic volume (ESV), **(B)** intraventricular septum diameter (IVSd) and left ventricular posterior wall diameter (LVPWd), **(C)** end-diastolic left ventricular internal diameter (LVIDd), **(D)** left ventricular ejection fraction (EF), and **(E)** global longitudinal strain (GLS) were assessed by transthoracic echocardiography in canines undergoing doxorubicin (DOX) therapy (n = 8). **Asterisks** indicate significant change compared with baseline measurements.

(intraclass correlation coefficient: 0.86; 95% confidence interval: 0.75 to 0.92; $p < 0.001$) (Figure 2A). Bland-Altman statistics showed no significant bias and good agreement between REST-1 and REST-2 diameter measurements (bias: 0.02 mm; 95% limits of agreement: -0.17 to +0.22 mm) (Figure 2B).

DOX-INDUCED CARDIOTOXICITY. Hemodynamics. In 8 canines, ADE and DOB elicited similar hemodynamic responses as were identified in control experiments, and these responses were not significantly influenced by DOX over time (Figure 3, Supplemental Table 2).

Echocardiography. End-systolic volume was significantly increased at ~12-mg/kg DOX (Figure 4A). LVEF was preserved until cumulative dosing of ~8 mg/kg of DOX therapy; thereafter, LVEF declined precipitously after higher doses were administered (Figure 4D). However, GLS was significantly reduced after ~4-mg/kg cumulative DOX therapy ($p = 0.011$) (Figure 4E).

Histopathology. Average severity of myocardial injury scores and histopathology for LV biopsies taken at ~4-mg/kg DOX and ~8-mg/kg DOX and at terminal necropsy showed the expected progressive increase in myocardial damage over time reflected by representative hematoxylin and eosin photomicrographs for each time point (Figure 5).

Vascular reactivity on CTA. Similar to GLS, ADE vasodilator responses were impaired as compared with REST-1, after only ~4-mg/kg cumulative dose of

DOX (LAD: -3 ± 1%, LCx: 0 ± 2%, RCA: -5 ± 2%) (**Figure 6**, Supplemental Table 3). In contrast, DOB-induced responses remained preserved, as compared with REST-2 (LAD: 18 ± 4%, LCx: 11 ± 3%, RCA: 11 ± 2%) at this time point (**Figure 6**, Supplemental Table 3). At a cumulative DOX dose of ~8 mg/kg, ADE vasodilator responses remained impaired (LAD: -3 ± 1%, LCx: 0 ± 1%, RCA: -2 ± 2%), and DOB dilation began to decrease (LAD: 4 ± 2%, LCx: 8 ± 3%, RCA: 3 ± 2%). At the terminal time point (12 to 15 weeks), we were able to assess coronary vasoreactivity in only 4 dogs due to hemodynamic instability related to DOX-induced cardiotoxicity. In these 4 canines, both ADE-induced (LAD: -3 ± 2%, LCx: -1 ± 1%, RCA: -2 ± 1%) and DOB-induced (LAD: 1 ± 2%, LCx: 1 ± 1%, RCA: 1 ± 1%) responses were impaired.

DISCUSSION

This study used a novel CT methodology to demonstrate impaired ADE- and DOB-induced coronary vasoreactivity in a chronic large animal model of DOX-induced cardiotoxicity. We demonstrate that noninvasive coronary CTA can provide a reliable assessment of epicardial coronary diameters during ADE- and low-dose DOB-induced coronary dilation, thus providing additional functional information regarding coronary vasoreactivity to be derived from noninvasive contrast CT angiography. In addition, the application of this method in the setting of progressive DOX chemotherapy administration indicates that an impairment in ADE-induced vasodilator responses occur early in the progression of anthracycline-induced cardiotoxicity (**Central Illustration**).

ADE promotes vasodilation in coronary microvascular beds by the activation of vascular smooth muscle A2 receptors. This arteriolar and pre-arteriolar vasodilation causes a reduction in vascular resistance, which in turn increases blood flow in larger vessels and elicits endothelial-dependent flow-mediated vasodilation in the epicardial vessels (25). On the other hand, DOB-induced vasodilation is thought to be a net effect of multiple vasodilator forces that include the stimulation of vascular β_2-adrenoreceptors leading to direct epicardial vasodilation and the release of vasodilatory metabolites because of greater inotropy or chronotropy of cardiomyocytes secondary to β_1-adrenoreceptor stimulation (26,27). In addition, DOB has been described to have α_1-adrenoreceptor agonist effects (27). Some DOB metabolites can also exert significant α_1-adrenoreceptor antagonist effects, which may contribute to coronary vasodilation (27). These presumed mechanisms are summarized in **Figure 7** and discussed in more detail subsequently.

In our studies for methodological development and assessment of reproducibility, we were able to detect significant epicardial coronary dilation after both ADE and DOB administration. In line with these findings, a previous study employing quantitative coronary angiography detected similar magnitudes of epicardial coronary vasodilation in response to DOB (19 ± 3% in normal and 8 ± 2% in mildly atherosclerotic epicardial segments) (28). Notably, canines usually have left-dominant coronary circulation, which may explain the relatively smaller diameter changes of the RCA in response to pharmacological stress compared with left-sided epicardial coronary diameters.

Quantitative CTA has been applied in clinical studies to improve the prediction of functionally significant coronary lesions in patients with suspected CAD (29). Prior studies have shown that the diagnostic performance of CTA can be greatly improved with incorporation of functional assessment, such as using computational modeling for the calculation of CT fractional flow reserve (30). In the current project, we applied a unique strategy for functional testing of coronary vasomotor function by utilizing coronary CTA for the quantitative measurement of epicardial coronary vasodilation in response to commonly used pharmacological stress agents.

There has been growing emphasis on identifying functional, molecular, and imaging biomarkers of cardiotoxicity that either precede or predict an impairment in LVEF. Measurement of GLS by 2-dimensional TTE has been proposed for this purpose (31,32). Along these lines, we detected reduced GLS at an early time point in our chronic canine model of DOX-induced cardiotoxicity. A good correlation between myocardial strain and coronary flow reserve has been demonstrated in patients presenting with acute myocardial infarction (33), and changes in coronary flow reserve have been shown to have a significant relationship with improvement in strain following percutaneous coronary intervention (34). Whether there is a temporal or causal relationship between myocardial strain and coronary vasomotor responses has yet to be elucidated. Also, the potential additive (or synergistic) value of CT imaging of vasoreactivity with GLS imaging is unable to be fully realized in this study, given the small sample size, but is indeed worth further study. Beyond GLS, other echocardiographic indices, such as indices of diastolic dysfunction, have been shown to precede declines in systolic function in some studies, although

FIGURE 5 Histology Assessment of Myocardial Biopsy and Autopsy Specimens

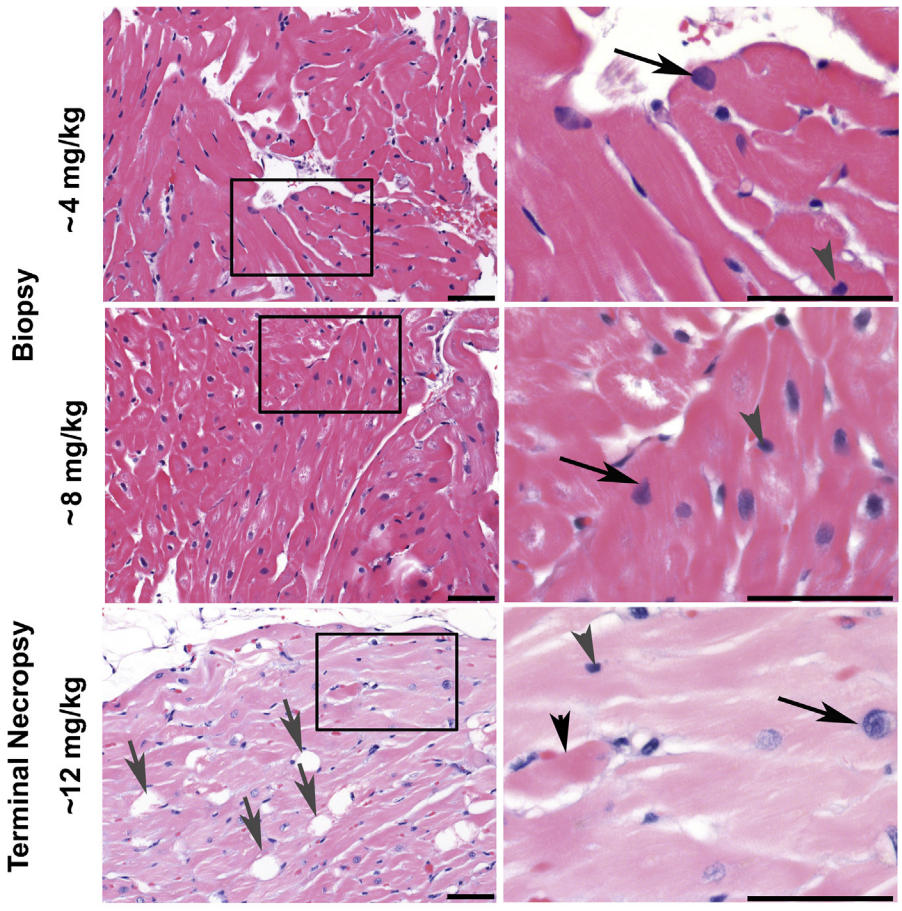

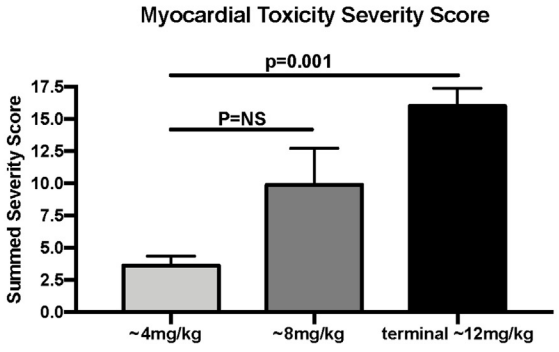

(Top) Representative hematoxylin and eosin photomicrographs in a canine model of chronic DOX cardiotoxicity show the average severity of myocardial injury increases with dose over time within the left ventricle. Biopsies collected at ~4 mg/kg and ~8 mg/kg and the terminal time point show scattered shrunken **(gray arrowhead)** and hypertrophied **(black arrows)** tissue at each time point; however, cardiomyocyte vacuolation **(gray arrows)** and hypereosinophilic cytoplasm **(black arrows)** are common at the terminal necropsy time point. **(Bottom)** Myocardial toxicity severity score in biopsy specimens and terminal autopsy samples with different cumulative doses of doxorubicin.

FIGURE 6 Rest-Stress Computed Tomography Angiography Analysis

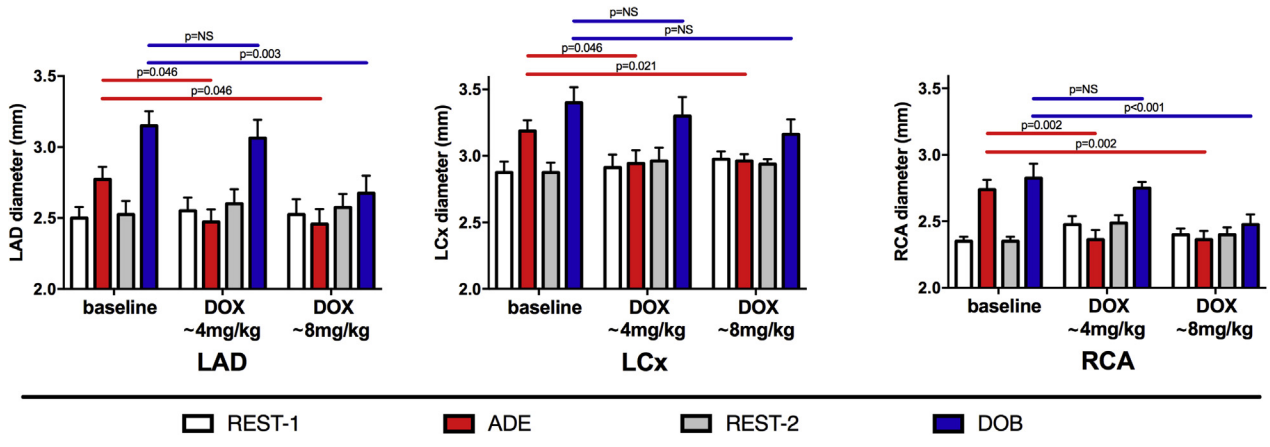

Coronary diameters (n = 8 in each group) in the left anterior descending coronary artery (LAD), left circumflex coronary artery (LCx), and right coronary artery (RCA) at baseline and after ~4 mg/kg and ~8 mg/kg of cumulative intravenous doxorubicin (DOX) treatment. Coronary diameters were assessed at rest (REST-1), in response to adenosine (ADE), at rest 30 min after discontinuation of ADE (REST-2), and during dobutamine (DOB) infusion.

reproducibility can limit the routine use of these indices for clinical decision making (35). Cardiac magnetic resonance imaging has also been tested in animal models (36,37), and T2-weighted imaging to detect edema and T1-weighted imaging to identify early fibrosis have been applied to patients receiving anthracyclines (38), but results have been mixed. In addition, several nuclear imaging approaches have shown promise in preclinical and small clinical studies, such as tracers targeting apoptosis (39), reactive oxygen species production (24), altered fatty acid oxidation (40), and altered sympathetic innervation (41), but these findings have yet to be confirmed in larger clinical studies.

To our knowledge, our study is the first to use a CTA approach for the early detection of DOX-induced cardiotoxicity. A prior small study that retrospectively investigated the clinical value of CTAs in cancer patients found that the imaging results influenced therapeutic management decision making in more than one-half of the patients studied (12). This study did not report on prior anthracycline use and did not comment on the utility of CTA for the early detection of DOX-induced cardiotoxicity. Our results extend these findings and indicate that in addition to excluding CAD, contrast-enhanced CT offers simultaneous information on coronary vasoreactivity, which may be used for the assessment of DOX-associated micro- and macrovascular injury and cardiotoxicity. Notably, the use of newer-generation CT cameras coupled with novel software can be used to measure other anatomical and physiological metrics, such as atrial and LV dimensions or volumes, LVEF, LV strain, and myocardial perfusion. These may also aide in clinical decision making in the context of DOX-related cardiotoxicity and in other cardiac pathologies.

Our results indicate an early chemotherapy-induced impairment in epicardial vasodilation that precedes the development of a significant decline in LVEF and substantial histopathological changes. Limited evidence suggests that DOX treatment can lead to a reduction in coronary blood flow; however, it is unclear whether this is a direct toxic effect on vascular endothelium or secondary to myocardial injury (42). In line with our observation, a recently published study found a modest but significant reduction in ADE coronary flow reserve as assessed by Rubidium-82 positron emission tomography in lymphoma patients shortly after DOX exposure (43).

In our experiments, the DOX-induced reduction in epicardial vasodilator responses was more apparent with ADE administration. The differential timing of impairment in vasodilator responses for ADE and DOB might provide some insight into the mechanism of DOX-induced impairment in epicardial vasodilation. Specifically, it is established that ADE-induced epicardial coronary responses rely on flow-mediated vasodilation, which is dependent on endothelial nitric oxide secretion that result from increases in flow-mediated shear stress (25). In contrast, DOB-induced vasodilation is, at least in part, achieved by direct

CENTRAL ILLUSTRATION **Impaired Vasoreactivity in DOX-Induced Cardiotoxicity**

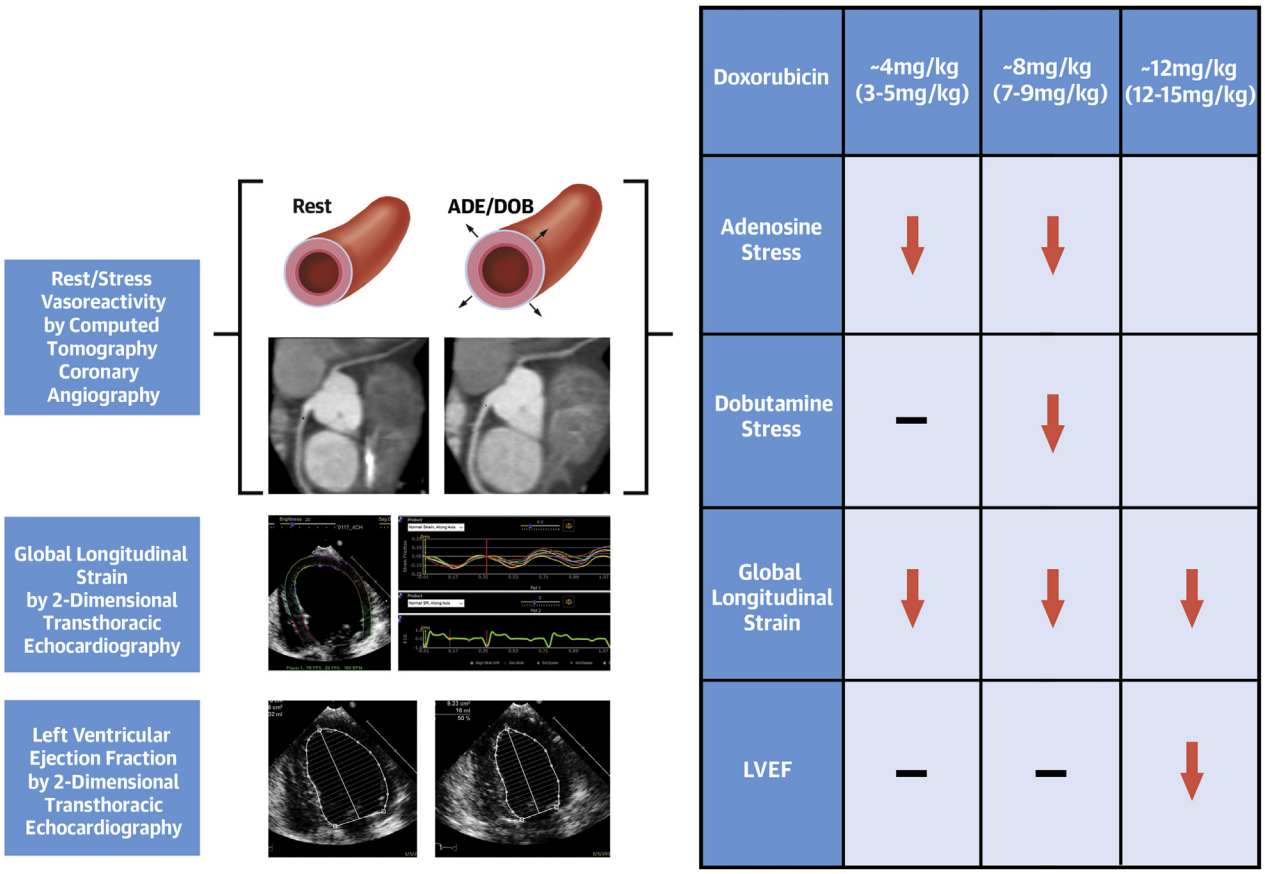

Feher, A. et al. J Am Coll Cardiol CardioOnc. 2020;2(2):207–19.

This study used a novel computed tomography (CT) methodology to demonstrate impaired adenosine (ADE)- and dobutamine (DOB)-induced coronary vasoreactivity in a large animal model of chronic doxorubicin (DOX)-induced cardiotoxicity. Left ventricular ejection fraction (LVEF) was not reduced until a cumulative DOX dose of 12 to 15 mg/kg was administered. Impairment in ADE-induced vasodilator responses occurred early in the progression of DOX-induced cardiotoxicity similar to impairment in global longitudinal strain (GLS). 2D = 2-dimensional; TTE = transthoracic echocardiography.

stimulation of myocardial and vascular β-adrenergic receptors (**Figure 7**) (26). DOX has been associated with a reduction in nitric oxide production in both animal models and human studies, resulting from endothelial nitric oxide synthase uncoupling (44–47). In addition, functional measures of endothelial dysfunction have been detected in childhood cancer survivors when compared with control subjects, including reduced flow-mediated brachial artery vasodilation, and increased carotid or femoral artery intima-media thickness (48,49). DOX has also been reported to diminish the binding affinity of agonists to the myocardial beta-receptors, which can potentially contribute to reduced vasodilator response to DOB (50). Therefore, our results may indicate the susceptibility of the endothelium to DOX that results in an early impairment in endothelium-dependent coronary vasodilation. However, this hypothesis needs to be tested in an experimental setting. As of now, it is unclear whether the impaired coronary vasodilation is only an indicator of cardiotoxicity or actively participates in the pathogenesis of DOX-induced cardiotoxicity.

By providing information about impaired coronary vasoreactivity, our novel method might complement other methods for the early identification of DOX-induced cardiotoxicity. Future preclinical studies with more frequent sampling during the early phases of DOX may reveal the specific timing of impairment in coronary vasoreactivity. The clinical safety of CT

FIGURE 7 Schematic Representation of ADE and DOB-Induced Epicardial Vasodilation

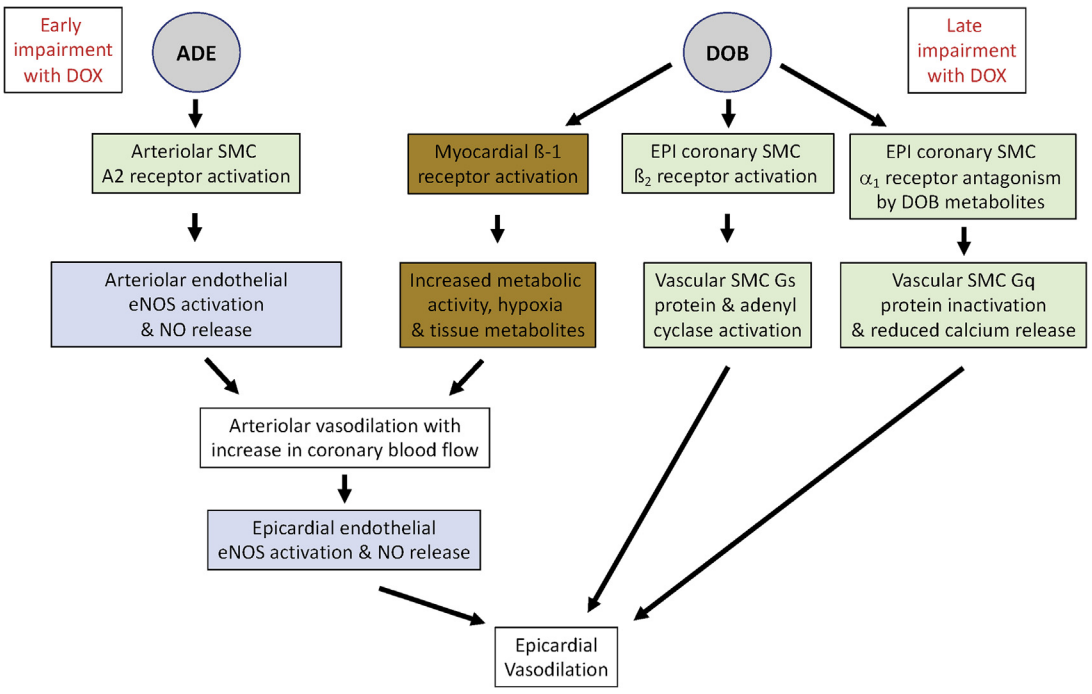

Blue coloring indicates primarily endothelial-mediated processes, **green coloring** primarily smooth muscle–mediated processes, and **brown coloring** primarily cardiomyocyte-mediated processes. A2 = adenosine receptor 2; ADE = adenosine; DOB = dobutamine; DOX = doxorubicin; eNOS = endothelial nitric oxide synthase; Gq = G protein q; Gs = G protein s; NO = nitric oxide; SMC = smooth muscle cell.

myocardial perfusion imaging has been well documented in the literature (51); however, prospective clinical studies are warranted to: 1) demonstrate the reproducibility of stress-induced coronary diameter measurements in clinical practice; 2) test whether coronary vasoreactivity is indeed an early independent predictor of DOX-induced cardiotoxicity; and 3) to assess whether it provides incremental value in addition to other traditionally used markers of DOX cardiotoxicity.

STUDY LIMITATIONS. The results of this study should be considered in the context of its limitations. First, routine clinical protocols often include nitroglycerin administration, which promotes vasodilation. Sublingual nitroglycerin administration has been shown to be associated with better image quality, improved diagnostic accuracy, and improved evaluation of coronary segments (52). However, our approach prohibits the administration of nitroglycerin, as it would eliminate the vasodilator reserve required to assess ADE or DOB vasoreactivity. Performing contrast CTA pre- and post-nitroglycerin administration may potentially provide further insight regarding the direct toxic effects of DOX on epicardial vessel reactivity. Second, the animals in our experiments were under general anesthesia, which may affect coronary vascular diameters and vasoreactivity. Third, the lack of control animals undergoing study procedures without DOX administration is a limitation of our study. However, during our analysis, we compared vasoreactivity results in DOX-treated animals with vasoreactivity measurements before and after DOX administration and used these baseline measurements as their own controls. Fourth, our approach requires both baseline and stress imaging, as well as serial assessments, thus leading to increased contrast administration and radiation exposure. Radiation exposure can be significantly decreased with reduced tube potential, prospectively gated electrocardiogram-triggered axial scan protocols, and iterative image reconstruction strategies, but radiation exposure with CT still remains a significant concern. Of note, this limitation is less relevant in preclinical experimental settings. Last, the use of stressor agents might lead to increased HR, which might compromise image quality. However, we analyzed the proximal coronary segments for detecting vasoreactivity in our experiments, and

these segments remained interpretable even at higher HRs.

CONCLUSIONS

Our results indicate that CTA can provide reliable assessment of epicardial coronary vasoactive responses to commonly used pharmacological stress agents. Our data also suggest that DOX is associated with an early impairment in ADE-induced vasodilation that occurs well before an impairment in LVEF. Larger clinical studies are needed to confirm our findings. In conclusion, studying coronary vascular reactivity might provide additional mechanistic insight and predictive information regarding anthracycline-induced cardiotoxicity.

ACKNOWLEDGMENTS The authors acknowledge the assistance of the Yale University veterinarian staff and residents as well as acknowledge the staff of the Yale Animal Research Center to ensure the health and well-being of the animals in this study. The authors also acknowledge the technical assistance of Tsa Shelton and Daniela Orozco from the Yale Translational Research Imaging Center, and also the assistance of Dr. Kim Smolderen, for helping with statistical analysis.

ADDRESS FOR CORRESPONDENCE: Dr. Albert J. Sinusas, Section of Cardiovascular Medicine, Yale University School of Medicine, P.O. Box 208017, Dana 3, New Haven, Connecticut 06520-8017. E-mail: albert.sinusas@yale.edu. Twitter: @attilafehermd.

PERSPECTIVES

COMPETENCY IN MEDICAL KNOWLEDGE: The vascular endothelium is emerging as a novel target for improving the detection, management, and prevention of DOX-induced cardiotoxicity. Noninvasive coronary CTA can provide a reliable assessment of epicardial coronary dilation during ADE and low-dose DOB. In our chronic canine model of DOX cardiotoxicity, we observed an early impairment in ADE-induced vasodilation that occurred prior to an impairment in LVEF. Our findings suggest that abnormalities in coronary vasoreactivity occur with DOX cardiotoxicity.

TRANSLATIONAL OUTLOOK: CTA imaging of vasoreactivity may be another sensitive tool for the early detection of DOX-induced cardiotoxicity. Experiments in our large animal model suggest that CTA can provide reliable assessment of epicardial coronary vasoactive responses, and this can potentially be useful in the early diagnosis of DOX cardiotoxicity. The clinical safety of CT myocardial perfusion imaging has been well documented in the literature; however, prospective clinical studies are needed to: 1) demonstrate the reproducibility of stress-induced coronary diameter measurements in clinical practice; 2) test whether coronary vasoreactivity is indeed an early independent predictor of DOX cardiotoxicity; and 3) assess whether it provides incremental value to other traditionally used markers of DOX cardiotoxicity.

REFERENCES

1. Hashim D, Boffetta P, La Vecchia C, et al. The global decrease in cancer mortality: trends and disparities. Ann Oncol 2016;27:926–33.

2. Oikonomou EK, Athanasopoulou SG, Kampaktsis PN, et al. Development and validation of a clinical score for cardiovascular risk stratification of long-term childhood cancer survivors. Oncologist 2018;23:965–73.

3. Yeh ET, Bickford CL. Cardiovascular complications of cancer therapy: incidence, pathogenesis, diagnosis, and management. J Am Coll Cardiol 2009;53:2231–47.

4. Von Hoff DD, Layard MW, Basa P, et al. Risk factors for doxorubicin-induced congestive heart failure. Ann Intern Med 1979;91:710–7.

5. Cardinale D, Colombo A, Bacchiani G, et al. Early detection of anthracycline cardiotoxicity and improvement with heart failure therapy. Circulation 2015;131:1981–8.

6. Cardinale D, Colombo A, Lamantia G, et al. Anthracycline-induced cardiomyopathy: clinical relevance and response to pharmacologic therapy. J Am Coll Cardiol 2010;55:213–20.

7. Hamo CE, Bloom MW, Cardinale D, et al. Cancer therapy-related cardiac dysfunction and heart failure: part 2: prevention, treatment, guidelines, and future directions. Circ Heart Fail 2016;9:e002843.

8. Ewer MS, Ali MK, Mackay B, et al. A comparison of cardiac biopsy grades and ejection fraction estimations in patients receiving Adriamycin. J Clin Oncol 1984;2:112–7.

9. Yancy CW, Jessup M, Bozkurt B, et al. 2013 ACCF/AHA guideline for the management of heart failure: a report of the American College of Cardiology Foundation/American Heart Association Task Force on Practice Guidelines. J Am Coll Cardiol 2013;62:e147–239.

10. Andreini D, Pontone G, Pepi M, et al. Diagnostic accuracy of multidetector computed tomography coronary angiography in patients with dilated cardiomyopathy. J Am Coll Cardiol 2007;49:2044–50.

11. Bhatti S, Hakeem A, Yousuf MA, Al-Khalidi HR, Mazur W, Shizukuda Y. Diagnostic performance of computed tomography angiography for differentiating ischemic vs nonischemic cardiomyopathy. J Nucl Cardiol 2011;18:407–20.

12. Daher IN, Banchs J, Yusuf SW, Mouhayar E, Durand JB, Gladish G. Impact of cardiac computed tomographic angiography findings on planning of cancer therapy in patients with concomitant structural heart disease. Cardiol Res Pract 2011;2011:268058.

13. Kotamraju S, Konorev EA, Joseph J, Kalyanaraman B. Doxorubicin-induced apoptosis in endothelial cells and cardiomyocytes is ameliorated by nitrone spin traps and ebselen. Role of reactive oxygen and nitrogen species. J Biol Chem 2000;275:33585–92.

14. Monti M, Terzuoli E, Ziche M, Morbidelli L. The sulphydryl containing ACE inhibitor Zofenoprilat protects coronary endothelium from doxorubicin-induced apoptosis. Pharmacol Res 2013;76:171–81.

15. Majzner K, Wojcik T, Szafraniec E, et al. Nuclear accumulation of anthracyclines in the endothelium studied by bimodal imaging: fluorescence and Raman microscopy. Analyst 2015;140:2302–10.

16. Vasquez-Vivar J, Martasek P, Hogg N, Masters BS, Pritchard KA Jr., Kalyanaraman B. Endothelial nitric oxide synthase-dependent superoxide generation from adriamycin. Biochemistry 1997;36:11293–7.

17. Feng Q, Song W, Lu X, et al. Development of heart failure and congenital septal defects in mice lacking endothelial nitric oxide synthase. Circulation 2002;106:873–9.

18. Sacco G, Mario B, Lopez G, Evangelista S, Manzini S, Maggi CA. ACE inhibition and protection from doxorubicin-induced cardiotoxicity in the rat. Vascul Pharmacol 2009;50:166–70.

19. Rasanen M, Degerman J, Nissinen TA, et al. VEGF-B gene therapy inhibits doxorubicin-induced cardiotoxicity by endothelial protection. Proc Natl Acad Sci U S A 2016;113:13144–9.

20. Luu AZ, Chowdhury B, Al-Omran M, Teoh H, Hess DA, Verma S. Role of endothelium in doxorubicin-induced cardiomyopathy. J Am Coll Cardiol Basic Trans Science 2018;3:861–70.

21. Herman EH, Ferrans VJ. Reduction of chronic doxorubicin cardiotoxicity in dogs by pretreatment with (+/-)-1,2-bis(3,5-dioxopiperazinyl-1-yl)propane (ICRF-187). Cancer Res 1981;41:3436–40.

22. Stendahl JC, Parajuli N, Lu A, et al. Regional myocardial strain analysis via 2D speckle tracking echocardiography: validation with sonomicrometry and correlation with regional blood flow in the presence of graded coronary stenoses and dobutamine stress. Cardiovasc Ultrasound 2020;18:2.

23. Montgomery RR, Booth CJ, Wang X, Blaho VA, Malawista SE, Brown CR. Recruitment of macrophages and polymorphonuclear leukocytes in Lyme carditis. Infect Immun 2007;75:613–20.

24. Boutagy NE, Wu J, Cai Z, et al. In vivo reactive oxygen species detection with a novel positron emission tomography tracer, (18)F-DHMT, allows for early detection of anthracycline-induced cardiotoxicity in rodents. J Am Coll Cardiol Basic Trans Science 2018;3:378–90.

25. Lupi A, Buffon A, Finocchiaro ML, Conti E, Maseri A, Crea F. Mechanisms of adenosine-induced epicardial coronary artery dilatation. Eur Heart J 1997;18:614–7.

26. Hodgson JM, Cohen MD, Szentpetery S, Thames MD. Effects of regional alpha- and beta-blockade on resting and hyperemic coronary blood flow in conscious, unstressed humans. Circulation 1989;79:797–809.

27. Ruffolo RR Jr. The pharmacology of dobutamine. Am J Med Sci 1987;294:244–8.

28. Barbato E, Bartunek J, Wyffels E, Wijns W, Heyndrickx GR, De Bruyne B. Effects of intravenous dobutamine on coronary vasomotion in humans. J Am Coll Cardiol 2003;42:1596–601.

29. Rossi A, Papadopoulou SL, Pugliese F, et al. Quantitative computed tomographic coronary angiography: does it predict functionally significant coronary stenoses? Circ Cardiovasc Imaging 2014;7:43–51.

30. Min JK, Leipsic J, Pencina MJ, et al. Diagnostic accuracy of fractional flow reserve from anatomic CT angiography. JAMA 2012;308:1237–45.

31. Farsalinos KE, Daraban AM, Unlu S, Thomas JD, Badano LP, Voigt JU. Head-to-head comparison of global longitudinal strain measurements among nine different vendors: the EACVI/ASE inter-vendor comparison study. J Am Soc Echocardiogr 2015;28:1171–1181, e2.

32. Toro-Salazar OH, Lee JH, Zellars KN, et al. Use of integrated imaging and serum biomarker profiles to identify subclinical dysfunction in pediatric cancer patients treated with anthracyclines. Cardiooncology 2018;4:4.

33. Park SM, Hong SJ, Kim YH, Ahn CM, Lim DS, Shim WJ. Predicting myocardial functional recovery after acute myocardial infarction: relationship between myocardial strain and coronary flow reserve. Korean Circ J 2010;40:639–44.

34. Ojaghi-Haghighi Z, Abtahi F, Fazlolah S, Moladoust H, Maleki M, Gholami S. Coronary flow reserve, strain and strain rate imaging during pharmacological stress before and after percutaneous coronary intervention: comparison and correlation. Echocardiography 2011;28:570–4.

35. Russell RR, Alexander J, Jain D, et al. The role and clinical effectiveness of multimodality imaging in the management of cardiac complications of cancer and cancer therapy. J Nucl Cardiol 2016;23:856–84.

36. Jordan JH, D'Agostino RB Jr., Hamilton CA, et al. Longitudinal assessment of concurrent changes in left ventricular ejection fraction and left ventricular myocardial tissue characteristics after administration of cardiotoxic chemotherapies using T1-weighted and T2-weighted cardiovascular magnetic resonance. Circ Cardiovasc Imaging 2014;7:872–9.

37. Neilan TG, Coelho-Filho OR, Pena-Herrera D, et al. Left ventricular mass in patients with a cardiomyopathy after treatment with anthracyclines. Am J Cardiol 2012;110:1679–86.

38. Drafts BC, Twomley KM, D'Agostino R Jr., et al. Low to moderate dose anthracycline-based chemotherapy is associated with early noninvasive imaging evidence of subclinical cardiovascular disease. J Am Coll Cardiol Img 2013;6:877–85.

39. Bennink RJ, van den Hoff MJ, van Hemert FJ, et al. Annexin V imaging of acute doxorubicin cardiotoxicity (apoptosis) in rats. J Nucl Med 2004;45:842–8.

40. Saito K, Takeda K, Okamoto S, et al. Detection of doxorubicin cardiotoxicity by using iodine-123 BMIPP early dynamic SPECT: quantitative evaluation of early abnormality of fatty acid metabolism with the Rutland method. J Nucl Cardiol 2000;7:553–61.

41. Carrio I, Estorch M, Berna L, Lopez-Pousa J, Tabernero J, Torres G. Indium-111-antimyosin and iodine-123-MIBG studies in early assessment of doxorubicin cardiotoxicity. J Nucl Med 1995;36:2044–9.

42. Gharanei M, Hussain A, Janneh O, Maddock H. Attenuation of doxorubicin-induced cardiotoxicity by mdivi-1: a mitochondrial division/mitophagy inhibitor. PLoS One 2013;8:e77713.

43. Laursen AH, Elming MB, Ripa RS, et al. Rubidium-82 positron emission tomography for detection of acute doxorubicin-induced cardiac effects in lymphoma patients. J Nucl Cardiol 2018 Oct 8 [E-pub ahead of print].

44. Cole MP, Chaiswing L, Oberley TD, et al. The protective roles of nitric oxide and superoxide dismutase in adriamycin-induced cardiotoxicity. Cardiovasc Res 2006;69:186–97.

45. Finkelman BS, Putt M, Wang T, et al. Arginine-nitric oxide metabolites and cardiac dysfunction in patients with breast cancer. J Am Coll Cardiol 2017;70:152–62.

46. Octavia Y, Kararigas G, de Boer M, et al. Folic acid reduces doxorubicin-induced cardiomyopathy by modulating endothelial nitric oxide synthase. J Cell Mol Med 2017;21:3277–87.

47. Duquaine D, Hirsch GA, Chakrabarti A, et al. Rapid-onset endothelial dysfunction with adriamycin: evidence for a dysfunctional nitric oxide synthase. Vasc Med 2003;8:101–7.

48. Chow AY, Chin C, Dahl G, Rosenthal DN. Anthracyclines cause endothelial injury in pediatric cancer patients: a pilot study. J Clin Oncol 2006;24:925–8.

49. Brouwer CA, Postma A, Hooimeijer HL, et al. Endothelial damage in long-term survivors of childhood cancer. J Clin Oncol 2013;31:3906–13.

50. Robison TW, Giri SN. Effects of chronic administration of doxorubicin on myocardial beta-adrenergic receptors. Life Sci 1986;39:731–6.

51. Rochitte CE, George RT, Chen MY, et al. Computed tomography angiography and perfusion to assess coronary artery stenosis causing perfusion defects by single photon emission computed tomography: the CORE320 study. Eur Heart J 2014;35:1120–30.

52. Takx RA, Sucha D, Park J, Leiner T, Hoffmann U. Sublingual nitroglycerin administration in coronary computed tomography angiography: a systematic review. Eur Radiol 2015;25:3536–42.

KEY WORDS anthracycline, cardiomyopathy, CT angiography, diagnosis, imaging, preclinical study

APPENDIX For supplemental tables, please see the online version of this paper.